Hydrogen Bonding of Water to Phosphatidylcholine in the Membrane As Studied by a Molecular Dynamics Simulation: Location, Geometry, and Lipid−Lipid Bridging via Hydrogen-Bonded Water

Marta Pasenkiewicz-Gierula,*,†,‡ Yuji Takaoka,‡ Hiroo Miyagawa,‡ Kunihiro Kitamura,‡ and Akihiro Kusumi§

Department of Biophysics, Institute of Molecular Biology, Jagiellonian University, Krakow, Poland, Department of Molecular Science, Research Center, Taisho Pharmaceutical Co. Ltd., Omiya, Saitama 330, Japan, and Department of Life Sciences, Graduate School of Arts and Sciences, The University of Tokyo, Tokyo 153, Japan

Received: July 15, 1996; In Final Form: December 13, 1996[⊗]

Hydrogen (H-) bonding between water and phosphatidylcholine was studied using a molecular dynamics simulation of a hydrated phosphatidylcholine bilayer membrane in the liquid crystalline phase. A membrane in the liquid-crystalline phase composed of 72 L-α-dimyristoylphosphatidylcholine (DMPC) and 1622 water molecules was generated, starting from the crystal structure of DMPC. At the beginning of the equilibration process, the temperature of the system was raised to 550 K for 20 ps, which was effective in breaking the initial crystalline structure. The thermodynamic and structural parameters became stable after the equilibration period of 1100 ps, and the trajectory of the system obtained during the following 500 ps agreed well with most of the published experimental data. Each DMPC molecule forms 5.3 H-bonds with water, while only 4.5 water molecules are H-bonded to DMPC. The primary targets of water for the formation of H-bonds are the non-ester phosphate oxygens (4.0 H-bonds) and the carbonyl oxygens (∼1.0 H-bonds). Of DMPC's H-bonds, 1.7 are formed with water molecules that are simultaneously H-bonded to two different DMPC oxygens (bridging water). In effect, approximately 70% of the DMPC molecules are linked by water molecules and form clusters of two to seven DMPC molecules. Approximately 70% of the intermolecular water bridges are formed between non-ester phosphate oxygens. The rest are formed between non-ester phosphate and carbonyl oxygens. About half of the intermolecular water bridges are involved in formation of multiple bridges, where two DMPC molecules are linked by more than one parallel bridge. These results suggest a possibility that water bridges are involved in reducing head group mobility and in stabilizing the membrane structure. Non-ester phosphate oxygen of DMPC makes one, two, or three H-bonds with water, but two H-bonds are formed most often (≈60%). In the case where two H-bonds are formed on non-ester phosphate or carbonyl oxygens, the average geometry of H-bonding is planar trigonal (in the case of water oxygen with two H-bonds, geometry is steric tetragonal). When oxygen atoms form three H-bonds, the geometry of H-bonding is steric tetragonal both for non-ester phosphate and water oxygens. On average, H-bonds make nearly right angles with each other when two or three water molecules are bound to the same DMPC oxygen, but the distribution of the angle is broad.

Introduction

Water is an important constituent of biological membranes and is a key element in a variety of structural and functional roles that membranes play in living cells. For example, formation of the membrane structure itself depends on water.[1] The crystal structure of dimyristoylphosphatidylcholine (DMPC) is stabilized by the presence of four water molecules per two DMPC molecules,[2,3] which link DMPC molecules via hydrogen bonds (H-bonds) with the non-ester phosphate oxygens.[2] Membrane permeability of hydrophilic nonelectrolytes is facilitated by penetration of water into the hydrophobic region of the membrane,[4−8] and water−phospholipid interaction plays a key role in membrane adhesion.[9]

In spite of such importance of water−phospholipid interaction, it is not well understood, particularly in the liquid-crystalline phase, which is most relevant to biological membranes. This is largely due to technical difficulties in applying diffraction and spectroscopic techniques to membrane systems in the liquid-crystalline phase. These methods have provided only limited information and sometimes gave different conclusions. ^{2}H-NMR studies have shown that, in fully hydrated dipalmitoyl-L-α-phosphatidylcholine (DPPC) liposomes, there are about five water molecules per phosphatidylcholine (PC) which are strongly bound and form an inner hydration shell of the head group.[10−12] However, the exact nature of the strong binding of water molecules (involvement of H-bonds, for example) and the location of water with respect to various moieties in DMPC have not been known. Even the existence of H-bond interactions between water and phosphate or carbonyl groups in PC (model) membranes has been a controversial issue (see ref 13 and references therein).

The first principal objective in the present investigation is, thus, to analyze the interaction between water and the various groups of PC as precisely as possible with a special attention paid to formation of H-bonds between water and PC. Since we are interested in biological membranes, we concentrated our effort on membranes in the liquid-crystalline phase.

† Department of Biophysics.
‡ Department of Molecular Science.
§ Department of Life Sciences. Present address: Department of Biological Science, Graduate School of Science, Nagoya University, Chikusa-ku, Nagoya 464-01, Japan.
⊗ Abstract published in *Advance ACS Abstracts,* April 15, 1997.

S1089-5639(96)02099-3 CCC: $14.00

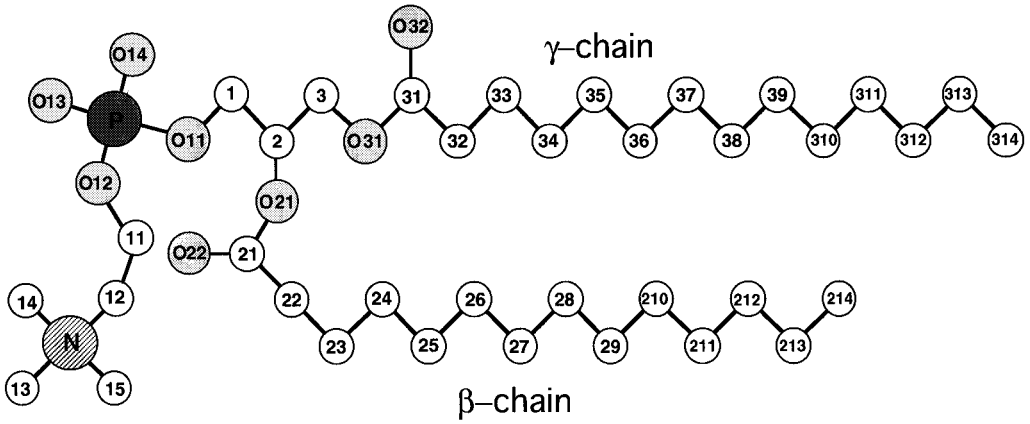

Figure 1. Atom numbering of DMPC.

Water molecules can cross-link neighboring PC molecules as exemplified in the crystalline structure, in which one-dimensional infinite DMPC−water ribbons are formed along a crystal axis.[2] In the liquid-crystalline phase, phase separation and microimmiscibility of lipids, formation of microclusters with short lifetimes, and cooperative movements of phospholipids have been reported.[14−18] Therefore, it is of interest and importance to examine a possibility of lipid cross-linking by H-bonding via a bridging water molecule, which may enhance the anomaly in mixing of lipids in the membrane. The second aim of this work is, thus, to study cross-linking of PC via water molecules in the liquid-crystalline phase, and if it exists, to study the conformation of the bridging structure.

An increasing number of reports is being devoted to the study of the phospholipid−water interface in the liquid-crystalline phase using molecular dynamics (MD) simulation. These studies have demonstrated that this method is well suited for understanding phospholipid−water interaction.[19−26] However, in most of these studies, phosphatidylethanolamine (PE) membranes have been used. Since (1) the interfacial properties of PE membranes differ greatly from those of PC membranes,[3,24] (2) PC is most abundant and is believed to form the basic structure of most of membrane systems in eukaryotic cells, and (3) we have been experimentally studying PC and PC−cholesterol membranes (for example, see refs 18−27, 27−32), the present work was undertaken to elucidate PC−water interaction in the liquid-crystalline phase.

In a recent report on the interfacial region of a monolayer of DMPC and water, Alper et al.[23] presented MD simulation data that support H-bonding of water to the phosphate and carbonyl groups. A clathrate structure of water from the first hydration shell of the choline group was found by these authors and Damodaran and Merz.[24] However, no details on the geometry of H-bonding was given.

In the present research, we analyzed the interaction between water and the head group of DMPC using a fully hydrated DMPC bilayer in the liquid-crystalline phase generated by MD simulation at constant temperature and pressure. Various structural and dynamic parameters obtained from the computer-generated DMPC bilayer are compared with those obtained from experiments published previously. The agreement of the parameters calculated from the simulated membrane with those measured experimentally was excellent. This warrants further examination of the simulated membrane to obtain other properties of the membrane (water−phospholipid interaction) that are impossible to be deduced experimentally. In the present work, the geometry of hydrogen bonds between water and non-ester phosphate oxygen atoms and carbonyl oxygen atoms (in the ester linkage between glycerol and acyl chains) has been characterized.

The most important finding in this work is perhaps that, even in the liquid-crystalline phase, a significant number of DMPC molecules (approximately 70%) are bridged with each other via water molecules that are simultaneously H-bonded to phosphate or carbonyl oxygens of two DMPC molecules. Such interaction resembles that in the DMPC crystal, although the bridges do not form an extended network and involve the carbonyl group. To our knowledge, water bridges between DMPC molecules in the liquid-crystalline phase have not been previously described.

Methods

1. Simulation System. Dimyristoylphosphatidylcholine (DMPC) membrane system consisting of 72 ($6 \times 6 \times 2$) DMPC molecules was constructed. The membrane was hydrated with 1622 water molecules and simulated for 1600 ps using Amber 4.0.[33] Figure 1 shows the structure and numbering of atoms in the DMPC molecule.

We began the simulations from the crystal structure. The asymmetric unit cell of the DMPC crystal consists of two DMPC molecules (DMPC A and B).[2] Molecule A is offset by 2.5 Å along the vertical axis relative to DMPC B, and their head groups have different conformations. The unit cell also contains four water molecules which are hydrogen bonded to DMPCs and form bridges between neighboring molecules. On the basis of X-ray diffraction data, Vanderkooi[34] built the "ideal" DMPC crystal and refined its structure by minimizing its energy in two arrangements: a multibilayer and a single bilayer. The conformations of DMPC A and B are similar in each arrangement. The only main difference is in the H-bond network: in the first arrangement, one of the water molecules forms an inter−bilayer bridge, while in the second arrangement, all of the bridges are within the same layer.

To build the membrane, we used the minimized structures of DMPC A and B in the second arrangement.[34] To facilitate calculation of nonbonded interactions, each DMPC molecule was divided into six residues, which were chosen in such a way that the total electrostatic charge of the residue was close to zero and the integrity of its chemical groups was preserved.

By applying $P2_1$ symmetry, which has been found in the DMPC crystal,[2] a $6 \times 6 \times 2$ bilayer was built. To avoid bad contacts between atoms, the energy of the system was minimized, using the MINMD module of the AMBER program,[33] for the same force fields and partial atomic charges which were later used for the MD simulation (see below). After minimization, two 15 Å-thick layers of water that were equilibrated by the Monte Carlo simulation ("Monte Carlo" water) were added along the bilayer normal. A unit box of "Monte Carlo" water is provided with the AMBER program. Initially, 1022 water molecules was added. At this stage, the water did not mix with the head-group region. In the next step, only the energy of the

water was minimized. After minimization, the dimensions of the membrane without water were $26.25 \times 55.18 \times 53.87$ Å^3, while with water the last dimension increased to 83.20 Å. The surface area per DMPC was about 40.2 Å^2 and the tilt angle of the hydrocarbon chains was 17.9°. The geometry of the simulation box was such that the bilayer surface was in the *x*,*y*-plane and its normal was along the *z*-axis.

To compare the properties of H-bonding between different oxygen atoms in DMPC and water with those of H-bonding among water molecules, a pure water system was simulated under the same conditions as that of the membrane. The water box contained a similar number of water molecules (1639) as the membrane system (1622 water molecules). The simulation was carried out for over 200 ps.

2. Simulation Parameters. OPLS parameters[35] for DMPC and TIP3P[36] for water were used. The united atom approximation was applied to the DMPC molecule to reduce computation time (thereby OPLS was selected). The TIP3P potential treats water as a rigid molecule with three charges: two on the hydrogen atoms (0.417 each) and one on the oxygen atom (−0.834). Since the bonded interactions are not considered, the potential includes only two terms: the Coulombic interaction of each water charge and the Lennard-Jones interaction of only the oxygen atom. The two sets of energy parameters are compatible.

To calculate the atomic charges of the DMPC molecule, the quantum mechanical electrostatic potentials were first established and then fitted to the classical Coulombic energy function to obtain the point atomic charges (ESP charges). Quantum mechanical electrostatic potentials were calculated using the GAUSSIAN-90 program[37] at the 6-31G basis set level. The use of this basis set gives more accurate point charges than those given by STO-3G, which is more commonly used. Point charges were calculated using the ESPFIT program from the AMBER package. Electrostatic potentials were estimated for grid points on four Connolly layers[38] (surfaces at a distance of 1.4−2.0 van der Waals radii) with a 1 Å × 1 Å mesh. The potentials were then fitted to the Coulombic energy function to obtain the point charges. In this calculation, the whole polar part of the DMPC molecule, including the head group and both carbonyl groups, was one unit. Two other units were β and γ chains.

To check the extent of the contribution of different conformations to DMPC atomic charges, the charges were established independently for DMPC A and B in the crystal.[39,64] In addition, the charges were calculated for DMPC A and B taken from the membrane after a 100 ps simulation. The charges for all four conformations were similar (Table 1). Therefore, in subsequent calculations we used the values averaged over four conformations. In addition, we averaged over corresponding atoms belonging to the carbonyl groups, β- and γ-chains, pairs of ester and non-ester phosphate oxygens, and the three methyls of the choline group. The charges agreed well with those calculated by Chiu et al.[39a] for DMPC, by Charifson et al.[19] for dilauroylphosphatidylcholine (DLPC), and by Stouch and Williams[43] for glycerylphosphorylcholine (GPC). However, their absolute values were larger than those calculated by Damodaran and Merz[24] (1994) for DMPC with STO-3G basis set level.

As OPLS parameterizations were verified against ab initio calculations with the 6-31G basis set, the atomic charges obtained in the present calculation, with the same basis set, are expected to be consistent with the OPLS parameter set.

3. Simulation Conditions. Three-dimensional periodic boundary conditions employing the usual minimum image convention were used.

TABLE 1: Point Atomic ESP Charges Calculated at the 6-31G Basis Set Level for Atoms in DMPC in Four Conformations: DMPC A and B of the Crystal (Cr.A and Cr.B, Respectively) and the Liquid-Crystalline Phase (Lq.A and Lq.B, Respectively) of the Bilayer

DMPC atom	Cr.A	Cr.B	Lq.A	Lq.B	av[a]	av (ua)[b]
C22	−0.346	−0.286	−0.373	−0.307	−0.328	−0.050
	0.156	0.130	0.129	0.096	0.128	
H	0.156	0.130	0.129	0.096	0.128	
C21	0.784	0.828	0.862	0.820	0.823	0.830
O22	−0.558	−0.568	−0.666	−0.537	−0.582	−0.579
O21	−0.573	−0.551	−0.484	−0.445	−0.513	−0.475
C2	0.226	0.103	0.081	−0.236	0.043	0.204
H	0.115	0.132	0.208	0.192	0.161	
H	0.062	0.084	0.070	−0.001	0.053	
H	0.030	0.051	0.061	0.044	0.046	
O11	−0.781	−0.747	−0.767	−0.699	−0.748	−0.799
P	1.918	1.985	2.035	1.943	1.970	1.970
O14	−0.997	−1.019	−1.002	−1.045	−1.057	−1.028
O13	−0.965	−0.992	−1.061	−0.978	−0.999	−1.028
O12	−0.835	−0.839	−0.917	−0.814	−0.851	−0.799
C11	0.459	0.462	0.744	0.555	0.555	0.570
H	0.019	0.025	−0.014	−0.042	−0.003	
H	0.013	0.002	0.028	0.029	0.018	
C12	−0.319	−0.285	−0.487	−0.265	−0.339	0.014
H	0.210	0.201	0.179	0.183	0.193	
H	0.138	0.129	0.199	0.176	0.160	
N	0.201	0.224	0.284	0.046	0.188	0.189
C13	−0.289	−0.363	−0.431	−0.347	−0.357	0.203
H	0.221	0.240	0.204	0.184	0.212	
H	0.192	0.207	0.257	0.198	0.213	
H	0.137	0.160	0.166	0.180	0.160	
C14	−0.476	−0.527	−0.488	−0.474	−0.491	0.203
H	0.197	0.211	0.251	0.215	0.218	
H	0.204	0.216	0.205	0.213	0.209	
H	0.214	0.227	0.197	0.215	0.213	
C15	−0.515	−0.543	−0.457	−0.306	−0.455	0.203
H	0.212	0.217	0.197	0.194	0.205	
H	0.266	0.272	0.197	0.173	0.227	
H	0.207	0.216	0.198	0.166	0.196	
C3	−0.035	0.177	−0.168	0.016	−0.002	0.216
H	0.118	0.067	0.137	0.112	0.108	
H	0.105	0.048	0.146	0.142	0.110	
O31	−0.430	−0.434	−0.449	−0.440	−0.438	−0.475
C31	0.840	0.801	0.864	0.843	0.837	0.830
O32	−0.567	−0.578	−0.590	−0.573	−0.577	−0.579
C32	−0.339	−0.263	−0.356	−0.254	−0.303	−0.050
ϱ	0.190	0.107	0.137	0.121	0.138	
H	0.138	0.186	0.220	0.204	0.187	
C23−C213 and C33−C313			0.008	(ua)[a,c]		
C214, C314			−0.084	(ua)[a,c]		

[a] Charges are averaged over four conformations. [b] Charges are additionally averaged over corresponding atoms belonging to the β- and γ-chains, over pairs of ester and non-ester phosphate oxygens, and over the three methyls of the choline group. For CH, CH_2, and CH_3 groups, the united atom model (ua) is applied, in which charges on the hydrogen atoms are added to that of the carbon atom. [c] Charges are additionally averaged over all CH_2 and CH_3 groups belonging to the β- and γ-chains, and a united atom model is used.

The water molecule in the TIP3P model is rigid, and the SHAKE algorithm[39] was used to preserve its bond lengths. Fixing the bond length of the water molecule by SHAKE and using the united atom approximation for DMPC implies that the vibrational motion of bonds involving hydrogen atoms, whose period is about 10 fs, is ignored in the MD simulation. Therefore, the time step was set to 2 fs.[40]

For nonbonded interactions, a residue-based cutoff was employed with a cutoff distance of 12 Å. To reduce calculation time of nonbonded interactions, each DMPC was divided into six residues containing the following atoms and groups: (1) C214−C29; (2) C28−C23; (3) C22, O21, and C21; (4) O21, phosphate group, α-chain, choline group, and C3; (5) O31−

C34; (6) C35−C314 (see Figure 1). Each residue was chosen in such a way that the total electrostatic charge on the residue was close to zero and that the integrity of its groups was preserved. If all of the atoms in one residue are farther than 12 Å from all of the atoms in another residue, the residues are considered to be noninteracting. The list of nonbonded pairs was updated every 50 steps.

We also simulated the system by using Ewald summation[41] to evaluate Coulombic interactions for over 100 ps. The results are essentially the same as those obtained by employing a cutoff scheme.

Simulation was carried out at a constant pressure (1 atm) and a constant temperature (310 K) (37 °C), which is above the main phase transition temperature for the DMPC bilayer (∼23 °C). Temperature of the solute and solvent was controlled independently. Both the temperature and pressure of the system were controlled by the Berendsen method.[42] The relaxation times for temperature and pressure were set at 0.4 and 0.6 ps, respectively. Applied pressure was controlled anisotropically, where each direction was treated independently and the trace of the pressure tensor was kept constant (1 atm).

Results and Discussion

1. Approach Toward Thermally Equilibrated Membrane in the Liquid-Crystalline Phase. The initial configuration of the membrane was generated on the basis of the crystal structure of DMPC. In the crystal state, the surface area per molecule was about 40 Å^2 and the hydrocarbon chains assumed an all-trans conformation.

To break the membrane crystal structure, the temperature of the system was raised from the initial 10 to 750 K and the simulation was run for 10 ps under constant volume and temperature (Figure 2a). The temperature was then gradually lowered to 310 K and the dimensions of the simulation box were slowly rescaled: the dimensions were increased in the *x* and *y* directions to adjust surface area/DMPC for the liquid-crystalline state and were decreased in the *z* direction (only for the water molecules) to obtain bulk water density as close to 1.0 as possible. Between rescaling, the simulation was run under constant volume and temperature. After about 80 ps, the surface area reached 59 Å^2 (Figure 2b). At that time, another 600 water molecules were added to the system, temperature was kept at 310 K, and the pressure control was applied. From this point onward, the simulation was run under a constant pressure of 1.0 atm.

These conditions caused a rapid decrease in the surface area to about 55 Å^2 (Figure 2b). Nevertheless, we continued the simulation for 40 ps. At this stage, the average number of gauche conformations per chain was far below the experimental value of 3,[44] and the surface area per molecule remained at 55 Å^2. Therefore, we raised the temperature first to 500 K, where we maintained the system for 20 ps and 550 K for 20 ps. The temperature was then slowly lowered to 310 K. After another 300 ps (till 500 ps from the onset of simulation), the potential energy of the system became stable and the surface area per DMPC (61 ± 1 Å^2/DMPC) also became stable (Figure 2b). More discussion on the surface area is given in the next section. Simulation was continued for another 1100 ps (total 1600 ps).

Comparison of order parameter profiles obtained for different time periods (Figure 3) indicated that they converge only after about 1100 ps simulation time. The number of gauche conformations per chain stabilized at that time (2.9 gauche bonds per chain, Figure 2c). For these reasons in this paper we present the results obtained from the trajectory during 1100−1600 ps.

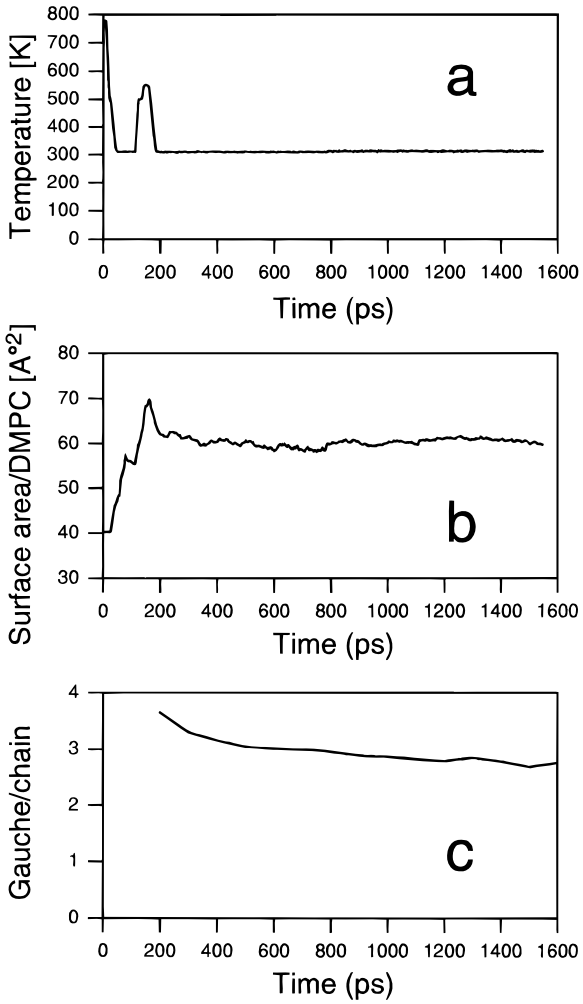

Figure 2. Diagrams showing the time developments of (a) temperature, (b) surface area per DMPC, and (c) the number of gauche bonds per chain.

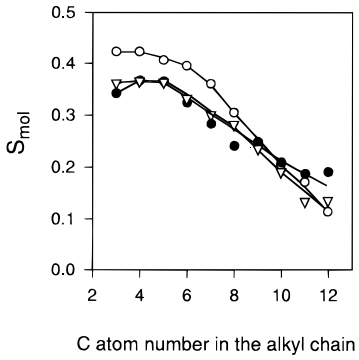

Figure 3. Time devlelopment of the profiles of the molecular order parameter. Keys: (○), 450−550 ps sample; (△), 1100−1200 ps sample; (●), 1500− 1600 ps sample.

During the equilibration period, the conformations, positions, and orientations of the DMPC head groups departed substantially from their initial states. In the DMPC single crystal the conformation of the head group α-chain is such that the α5 torsion (O12−C11−C12−N) (see Figure 1) is gauche$^+$ (g$^+$) (83.9° and 82.1° in DMPC A and B, respectively) and α4 torsion (P−O12−C11−C12) is trans (t) (198.1° and 191.6° in DMPC A and B, respectively).[39] In the simulated DMPC bilayer in the liquid-crystalline phase, the conformation of α5 changes to predominantly trans (79% of α5 is trans, 9% is gauche$^+$, and 9% is gauche$^-$ (g$^-$)), while that of α4 remains mainly trans (76% of cases). There are relatively fast transitions between

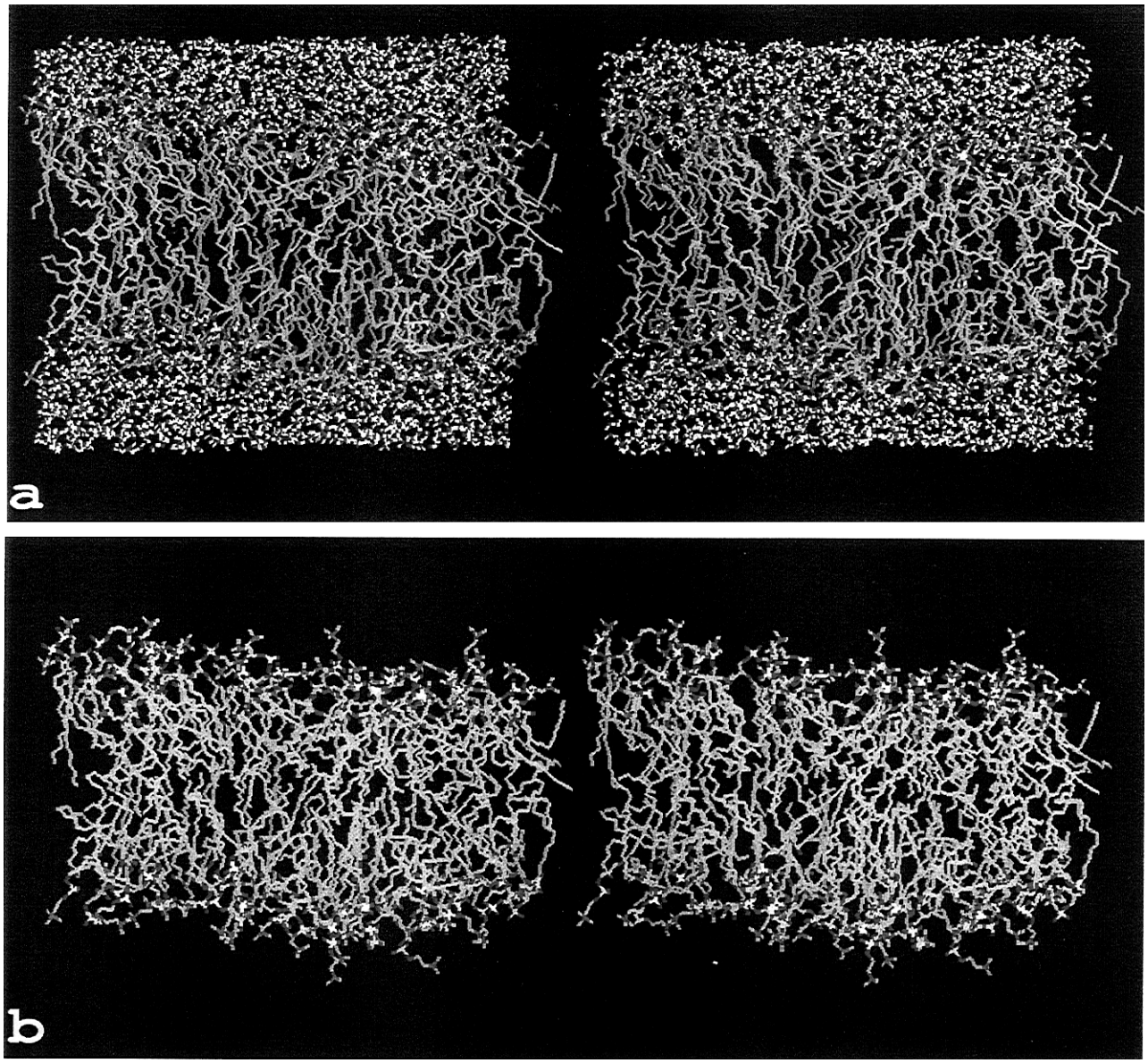

Figure 4. Snapshot of DMPC bilayer after 1500 ps equilibration: (a) the full system; (b) water is removed to show head-group conformation.

conformations of head groups. On average, for α5, gauche−trans isomerization occurs every 250 ps, while for α4, the isomerization occurs every 155 ps. Thus, during the simulation time, each DMPC head group changed its conformations many times. Also, due to the expansion of the surface area per DMPC from initial 40 Å^2 in the crystal phase to 61 Å^2 in the liquid-crystalline phase, the positions and orientations of the head groups changed. The average radial displacement of the center of mass of the head group in the *x*,*y*-plane during 1100 ps equilibration time is 13.6 Å. The initial orientation (in the DMPC crystal) of the P−N vector relative to the *x*-axis is −112° for DMPC A and 107° for DMPC B. In the liquid crystal, the orientations of the P−N vectors of DMPC A and B span a broad range of both negative and positive angles. It is concluded that the initial difference in the head groups of the two conformers is lost in the equilibrated membrane.

Figure 4 is a snapshot of the bilayer at 1500 ps.

2. Characterization of the Membrane Systems: Comparison with Experimental Data. We generated a fully hydrated DMPC bilayer system as a model of biological membranes. The system consists of 72 DMPC and 1622 water molecules. Thus, there are approximately 23 water molecules/DMPC in the system (∼38% by weight). Since between 23 and 28 water molecules/DPPC are present in fully hydrated multibilayers of DPPC,[10−12,45] and this number is smaller for DMPC multibilayers,[46] the number of water molecules present in our system is thought to be sufficient to fully hydrate the membrane.

The average surface area per DMPC in the simulated membrane was 61 ± 1 Å^2. Comparison of this number with experimental data is difficult because of poor agreement among experimental results regarding the surface area per phospholipid in the liquid crystalline state. The surface area/PC determined by X-ray diffraction and NMR ranges from 56 to 72 Å^2 for DMPC and DPPC membranes.[12,46,47] Nagle[12] identified errors associated with various methods for evaluation of surface area and then obtained a value of 62 ± 2 Å^2/DPPC using a formula which employed only NMR order parameters from the plateau region and the volume of the methylene group, which has been confirmed recently.[47a] The alkyl chains of DPPC are longer than those of DMPC by two methylene groups. The area/DMPC of 61 ± 1 Å^2 obtained in the present simulation is in good agreement with this value, as well as the surface area/DPPC of 61.8 Å^2 recently obtained by Tu, Tobias, and Klein,[47b] since the area/PC decreases with decreasing hydrocarbon chain length.[46] Meanwhile, Chiu et al. reported the surface area/

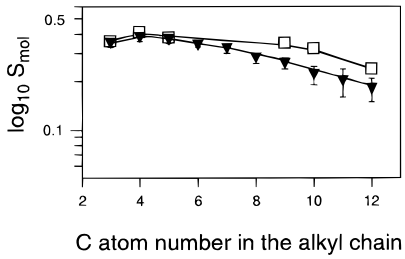

Figure 5. Molecular order parameter (S_{mol}) calculated for DMPC at 310 K (averaged over β- and γ-chains and over 500 ps) plotted against the carbon number in the alkyl chain (filled triangle) and that determined by ^{2}H-NMR for the DPPC bilayer at 333 K (open square).[50,51] Error bars are standard deviations (SD).

DMPC of 57.3 Å^2 on the basis of their MD simulation at a constant temperature of 325 K and with a lateral pressure set to −100 atm.[39a]

The number of gauche rotamers/myristoyl chain in our system at 37 °C is 2.9 ± 0.1. In the liquid-crystalline state, the average number of gauche conformations in the hydrocarbon chain of DMPC was estimated by Pink et al.[48] to be about 3.5. In more recent studies on DPPC bilayers using infra red spectroscopy and deuterated derivatives of DPPC, Mendelsohn et al.[44] obtained a range of 3.6−4.2 gauche rotamers/palmitoyl chain at 48 °C. In DMPC bilayers at 28 °C, the number of gauche rotamers/myristoyl chain was estimated to be 3.2.[49] Thus, the number of gauche rotamers/myristoyl chain in our systems (2.9 ± 0.1) is close to the experimental estimates. The profile of the order parameter indicates general agreement with that determined by ^{2}H-NMR for DPPC (Figure 5).[50] S_{mol} decreases exponentially toward the methyl terminal group of the alkyl chain as found by a spin-labeling method.[51]

The tilt angle of hydrocarbon chains with respect to the bilayer normal is almost zero in the equilibrium state in the computer model. In the initial structure of the bilayer, which was based on the crystal structure, the tilt angle was 17.9°. This equilibrium value is in good agreement with both experimental data[52,53] and theoretical calculations.[54]

Neutron diffraction on DPPC membranes has shown that the average orientation of the P−N vector is almost parallel to the membrane surface.[55] The vector has the same tendency in the simulated membrane, the average angle between the P−N vector and the surface plane is 16 ± 30°. The electron density profile of the bilayer agrees well with X-ray diffraction data (data not shown).[56]

The membrane thickness of the simulated membrane was estimated in three ways. The average N−N distance of 35.0 Å, the average P−P distance of 34.0 Å, and the distance between the points at which the atomic (electron) density of DMPC becomes half of its peak value of 37 ± 2 (37 ± 1) Å were obtained. These are in general agreement with 35.7 Å obtained experimentally in the liquid-crystalline phase.[46]

These results suggest that the simulated membrane reproduces well various properties of PC bilayers in the liquid-crystalline phase that have been observed experimentally. Therefore, we assume that the simulated membrane is a good model of DMPC membranes and that we can use it with some confidence to obtain information that is experimentally inaccessible, such as atomic-level structure and dynamics. In the present paper, we concentrate on H-bonding of water to DMPC.

3. Water Ordering by Various DMPC Groups. Figures 6a,b,c show the radial distribution functions (RDFs) of water oxygen atoms relative to DMPC oxygen atoms, namely those in non-ester phosphate (O14 and O13), ester phosphate (O11 and O12), carbonyl (O22 and O32), and glycerol (O21, O31)

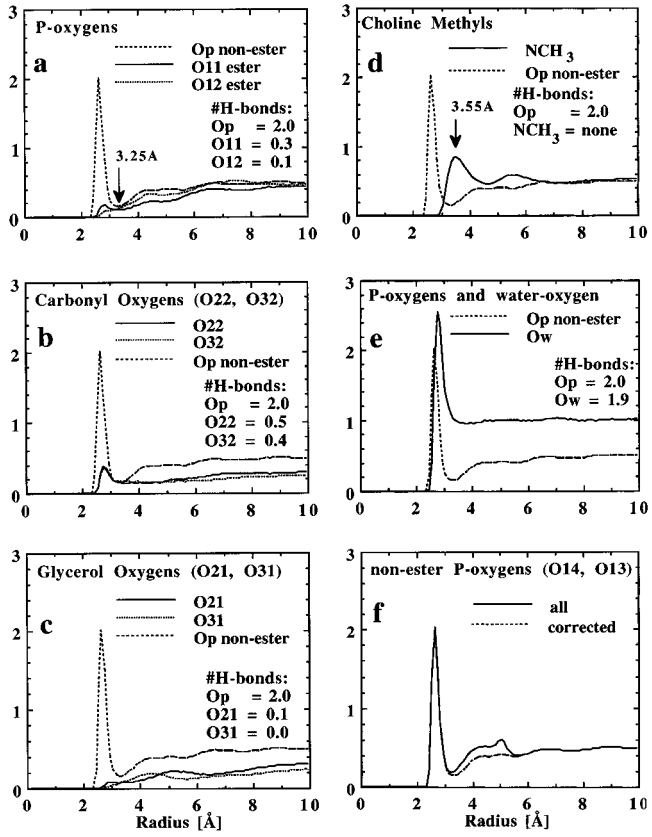

Figure 6. RDFs of water with respect to the oxygens of DMPC: (a) the phosphate group; (b) the carbonyl groups; (c) the glycerol group; (d) with respect to the choline methyl groups of DMPC; (e) with respect to the water oxygen. To facilitate comparison, the RDFs are shown together with the RDF for the non-ester phosphate oxygens (Op's: O14, O13). Due to strong ordering of water by the Op's, water that was H-bonded to these oxygens was excluded from the calculations of RDFs. RDFs before (solid line, all water) and after (broken line) correction are shown in (f) using Op as an example. (When calculating the RDF for O14 (O13), the water that was H-bonded to O13 (O14) was excluded from the calculations in the corrected case. After correction, the second peak in the distribution disappears.)

groups, respectively (the atomic numbering is shown in Figure 1). These RDFs show that, among all of the DMPC oxygens, by far the largest ordering of water is around the non-ester phosphate oxygens (Op). This ordering effect is visible to a much lesser extent around the carbonyl oxygens (Oc) and one of the ester phosphate oxygens, O11, whereas the other ester phosphate oxygen, O12, and the glycerol oxygens practically have no ordering effect on water.

The RDFs for oxygens in each of the pairs (O11 vs O12, O22 vs O32, O21 vs O31) differ slightly, indicating that the oxygens are not fully equivalent, except for in the O14−O13 pair. In the case of the carbonyl oxygens, this lack of equivalency probably occurs because the average position of O32, which belongs to the γ-chain, is located deeper within the nonpolar region of the membrane than O22, which belongs to the β-chain (Figures 1 and 8). Due to this nonequivalence, we analyzed H-bonding properties of each oxygen atom in each pair separately, except for the non-ester phosphate oxygens, which in most cases, we treated as equivalent atoms. In the following, we call these nonester phosphate oxygens (O13 and O14) collectively as Op, carbonyl oxygens (O22 and O32, when we call them collectively) as Oc, and the water oxygen as Ow.

The RDF of Ow relative to the choline methyl (NCH_3) groups, together with the RDF for Op, is shown in Figure 6d. The function has a distinct maximum at r = 3.55 Å. However, this maximum is not related to H-bonding: if it were, the

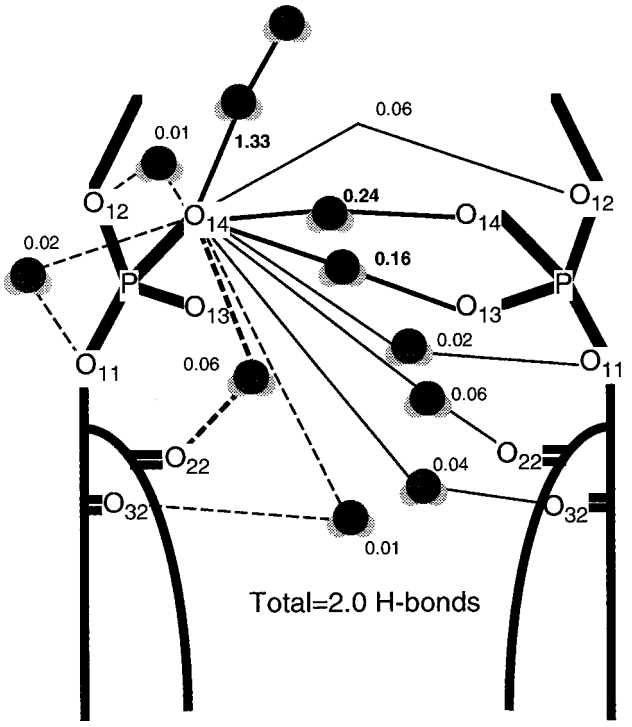

Figure 7. The partners with which an Op (represented by O14) is linked via a water cross-bridge. Expressed in the average number of H-bonds per case.

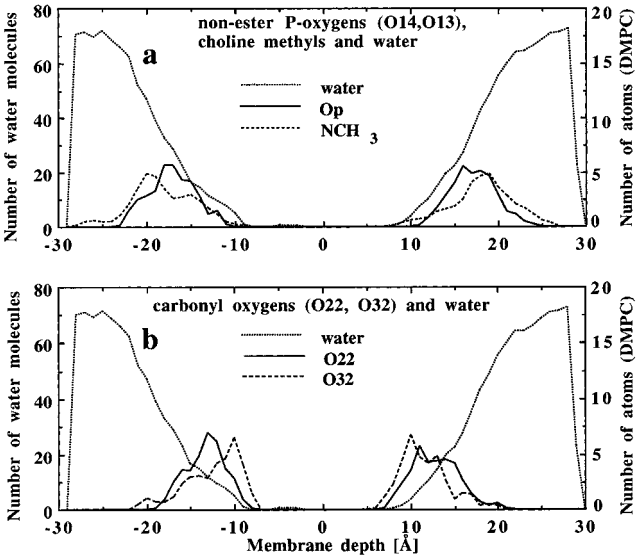

Figure 8. Density profiles of water oxygens shown together with (a) Op's and choline methyls and (b) carbonyl oxygens O22 and O32. Note that the ordinate scale for the DMPC atoms and groups was expanded by a factor of 4 compared with that for water to show their profiles more clearly.

maximum of the RDF would be for r less than 3 Å (the C−H bond length is 1.1 Å and the maximum of the RDF of the water oxygens relative to the NH_3 hydrogen atoms of DLPE corresponds to a distance of 1.8 Å,[22] which would give an expected maximum at 2.9 Å if H-bonds were formed). This result is consistent with the fact that the methyl group, a hydrophobic moiety, is not able to make H-bonds with water.[13,57]

For comparison, the RDF of water oxygens relative to a water oxygen was calculated for a pure water system and is shown in Figure 6e. The RDF of TIP3P water, which we used in the simulation, has only one peak at 310 K; its position corresponds to a distance slightly larger than that for Op's, indicating that

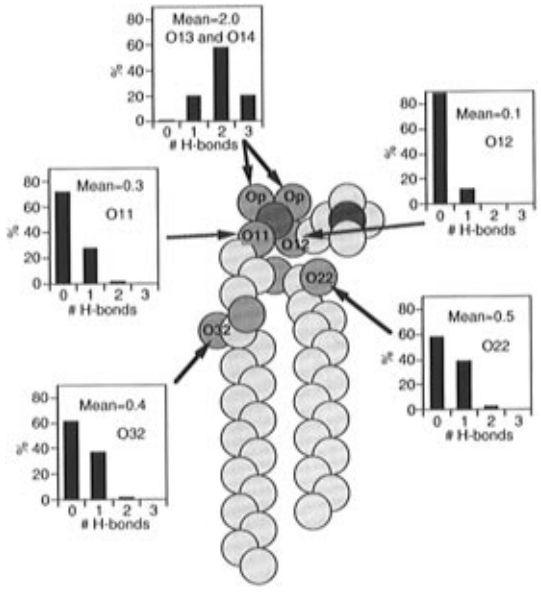

Figure 9. The mean number of water H-bonds formed on each DMPC oxygen. Distributions of the number of H-bonds on each DMPC oxygen are also shown.

the average length of H-bonds of the water oxygen is larger than that of the Op.

4. Numbers of H-Bonds and H-Bonded Water Molecules. We adopted the following geometric criteria for the H-bond: the distance between the water oxygen (Ow) and the DMPC oxygen is shorter than or equal to 3.25 Å (which is the position of the first minimum in the RDF of Op−Ow and Oc−Ow, Figure 6a,c) and the H-bond angle θ, which is the angle between the vector linking the DMPC and water oxygens and one of the H−Ow bonds of the water (Figures 12 and 13a), is less than or equal to 35°, as proposed by Raghavan et al.[21] This value is larger than the limiting value of about 20° encountered in a screening of the crystallographic data.[58] However, this value was used because due to the dense packing in the membrane, the deviation from linearity in H-bonding may be greater than that in an unrestricted environment.[21] The number of H-bonds made by a DMPC oxygen was determined by counting the number of water molecules that satisfy these geometric criteria and by averaging over time (500 ps) and over all of the DMPC molecules in the simulation system.

Each DMPC molecule makes 5.3 H-bonds with water (Table 2). The total number of H-bonded water molecules per DMPC is 4.5 ± 0.2 (Table 2), i.e., 18% [(5.3−4.5)/4.5] of the H-bonded water molecules are simultaneously bonded to two different DMPC oxygens to form either intramolecular or intermolecular bridges (see below).

The nearest-neighbor water of a DMPC oxygen is defined as any water molecule whose oxygen atom is within 3.25 Å (first minimum in the Op−Ow and Oc−Ow RDFs, see Figures 6a,c) from the DMPC oxygen. The total number of nearest-neighbor water molecules per DMPC is 4.8 (after correcting for cases in which the same water molecule is a nearest neighbor of other DMPC oxygens) (Table 2). This indicates that almost all [(4.5/4.8)(100)] = (94%) of the nearest-neighbor water molecules around DMPC oxygens form H-bonds. Formation of H-bonds between DMPC and water is consistent with the result of previous MD simulation by Alper et al.[23] and provides further support for the experimental data that indicated formation of water H-bonding with Op's and Oc's[13] (against the results that suggested no formation of H-bonds).

Only 6% difference between the number of H-bonded water molecules and that of nearest neighbors indicates that the above

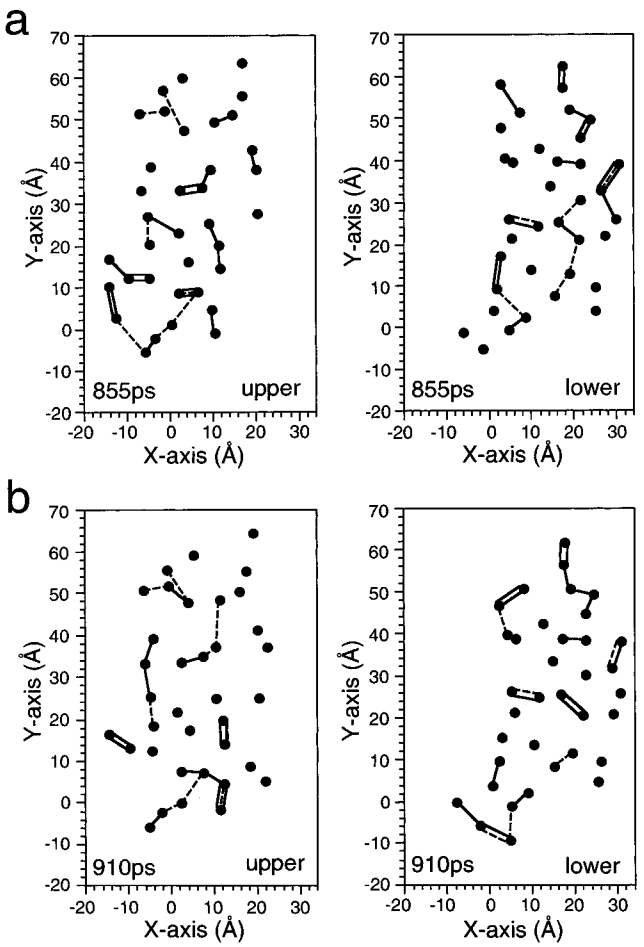

Figure 10. Cross-bridges of H-bonded water molecules between DMPC molecules at (a) 1100 ps and (b) 1155 ps. Each layer in the bilayer (upper and lower layers) are separately shown. Bridges that survived for more than 2 ps are displayed: (●), shows the *x* and *y* coordinates of the phosphorus atom; (solid line), Op−Op bridge; (broken line), Op−Oc bridge.

geometric criteria of H-bonding, instead of simple distance criterion, are not restrictive; using these criteria enables us to see the dynamic nature of H-bonding (to be published elsewhere).

The nearest-neighbor water of a choline methyl group is defined as any water molecule whose oxygen atom is within 4.75 Å from the methyl group, which is again based on the first minimum in the RDF of NCH_3−Ow (Figure 6d) and is not H-bonded to any Op. The total number of nearest neighbors per choline group is 7.6 (after correcting for cases in which the same water molecule is the nearest neighbor of other methyl groups) (Table 2). As stated above, the nearest-neighbor water of a choline methyl group does not form hydrogen bonds with the choline methyl groups.

The total number of "ordered" neighboring water molecules around DMPC can be estimated from the RDFs shown in Figure 6 by adding the number of the nearest-neighbor water of DMPC oxygens and choline methyl groups. The number of "ordered" water is 12−13/DMPC 4.5 of which form hydrogen bonds with DMPC oxygens. This number coincides well with the number of bound water per PC, estimated experimentally to be 11−16/PC.[59]

Experimental studies have also estimated that about five water molecules are strongly bound to a PC molecule[10,12] and could not be removed by a dehydrating reagent, poly(ethylene glycol).[11] This number is close to the number of nearest-neighbor water molecules of Op's and Oc's in the present estimate (4.8), 4.5 of which form H−bonds with DMPC. Therefore, we suggest that the strongly bound water observed in spectroscopic experiments are the water molecules that are H-bonded to DMPC oxygens. This agrees well with theoretical calculations of Frischleder et al.[60]

The fractions of H-bonds formed on each oxygen atom with respect to the total number of H-bonds (5.3 H-bonds) are also shown in Table 2. H-bonds on Op's account for 76% and on Oc's for 17% of the total number of H-bonds on DMPC. These together are responsible for 93% of H-bonds formed on DMPC.

About 32% of the H-bonds on DMPC oxygens share water molecules with other DMPC oxygens within the same DMPC (6.4% of the 5.3 H-bonds on a DMPC molecule) or in other DMPC molecules (25.4% of the 5.3 H-bonds on a DMPC molecule) (Tables 2 and 4). These results indicate that many intra- and intermolecular bridges via water molecules are formed within and between DMPC molecules, which is perhaps one of the most interesting results in this study and will be discussed in detail in sections 4 and 5b. (Conformations of various inter- and intramolecular bridges are shown in Figure 11.)

4a. H-bonds between Non-Ester P-Oxygen (Op: O14 and O13) and Water. Each Op forms an average of 2.0 H-bonds with water (Table 2), which constitute 38% of all H-bonds on DMPC (76% of H-bonds on a DMPC are on the two Op's). Each Op forms at least one H-bond with water (except 0.5% of the cases in which no H-bonds is formed with water). These oxygens most often form two H-bonds with water (∼60% of Op), less often form one or three H-bonds (∼20% each of Op), and rarely form four H-bonds (Table 3). Although cases of zero and four H-bonds can be found, they mostly show very short lifetimes (less an 0.2 ps).

About 30% of the bonds on Op's share water molecules with other DMPC oxygens within the same DMPC (3% of H-bonds on Op's) or in other DMPC molecules (25% of H-bonds on Op's) (Tables 2 and 4). Such inter- and intramolecular bridges via two H-bonds will be discussed in detail in sections 4 and 5b. The partners with which an Op (represented by O14) is linked via a water bridge are summarized in Figure 7.

It is interesting to note that the number of H-bonds the Op's form with water in the liquid-crystalline state is the same as that formed by the Op's of DMPC B in the crystal (which extends more toward the polar region of the membrane than DMPC A).[34] The Op's of DMPC A form one H-bond each. This smaller number of H-bonds made by DMPC A probably results from the fact that DMPC A is located deeper in the hydrophobic region in the membrane-like crystal structure.

4b. H-bonds between Ester P-Oyxgens (O11 and O12) and Water. In contrast to Op's, most (70%−90%) of the ester phosphate oxygens do not form H-bonds with water, as shown in Table 3. The numbers of H-bonds on ester phosphate-oxygens are 0.3 for O11 and 0.1 for O12 on average, representing only 6% and 2% of the total number of H-bonds formed on DMPC (Table 2). Almost 40% of the bonds share water with other DMPC oxygens, mainly with Op's of other DMPC molecules (Tables 2 and 4).

The ester phosphate oxygens and the glycerol oxygens have the same OPLS nonbonded parameters; their values are smaller than those for the non-ester and carbonyl oxygens, and thus they are expected to make H-bonds less readily. The glycerol oxygens have the smallest partial atomic charges (Table 1), so their H-bonding capabilities are lowest of all the DMPC oxygen atoms (Figure 6b).

4c. H-Bonds between Carbonyl Oxygens (Oc: O22 and O32) and Water. Carbonyl oxygens form H-bonds with water in approximately 40% of the cases (Table 3). O22 and O32 form

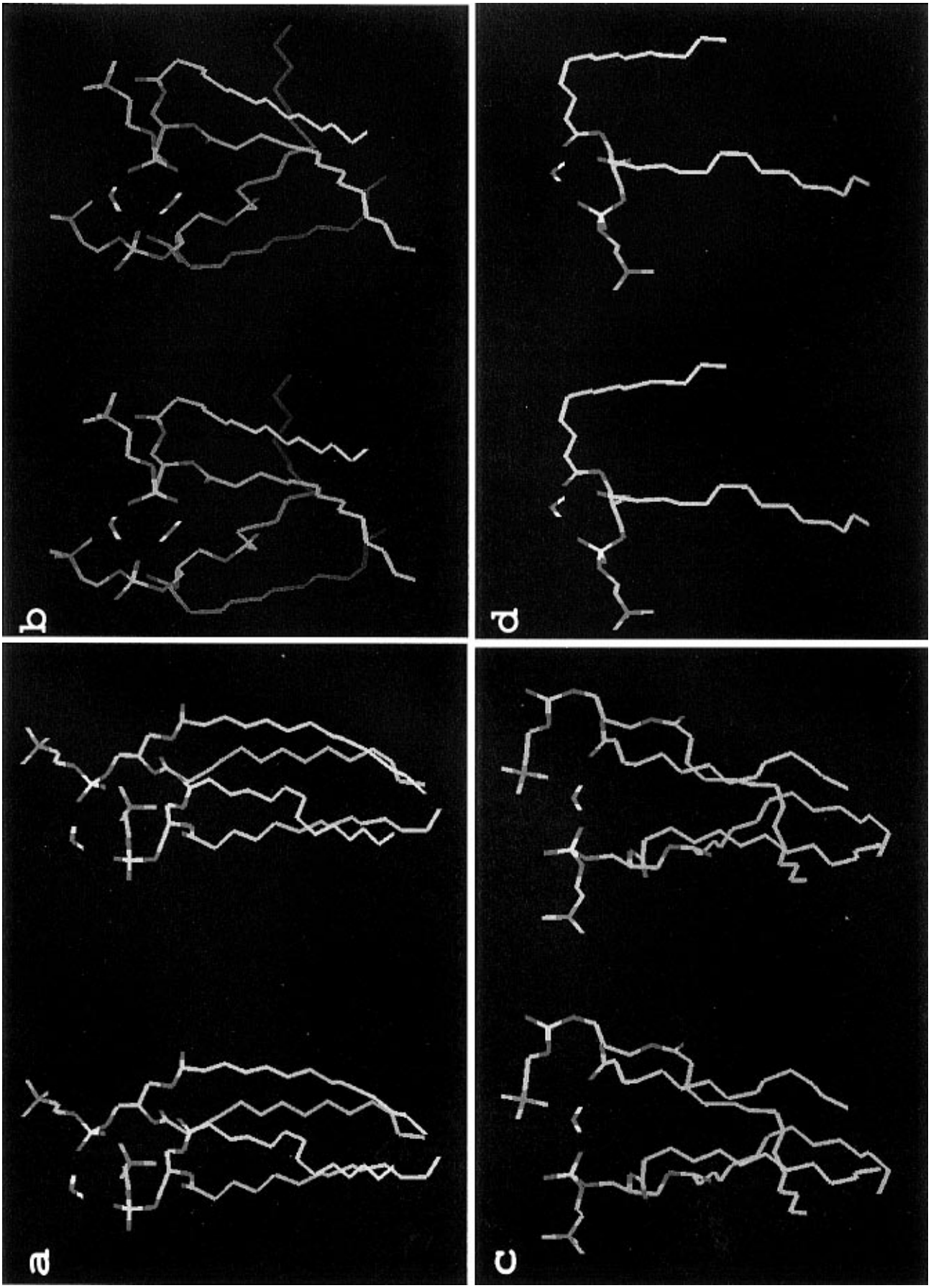

Figure 11. Stereoviews of representative water bridges: (a) Op−Op single bridge, (b) Op−Op double bridge, (c) Op−Oc intermolecular single bridge, (d) Op−Oc intramolecular single bridge.

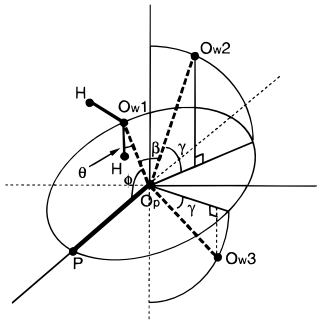

Figure 12. Definition of H-bond angles, θ, β, ϕ, and γ: (solid line), P−Op bond; (thick dash line), H-bond; (shaded plane), the plane determined by P, Op, and one of Ow of H-bonded water. The intersection of this plane and one of the sides of the tetragon is shown by a dash−dot line. Thick dot lines are to show the definition of γ angle (the angle between the shaded plane and the line Op−Ow). Thin dot lines show the bottom side of the tetragon to help the eye. For each Op, geometry is different and may not be symmetric about the P−Op axis.

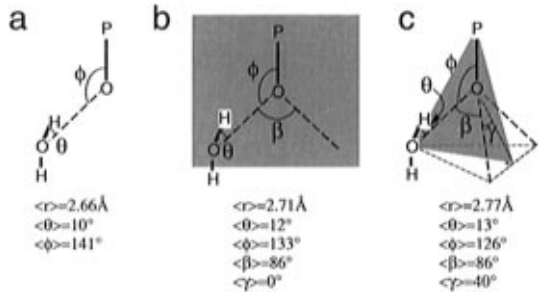

Figure 13. The average geometries of H-bonds (H-bonding criteria: $r \leq 3.25$ Å, $\theta \leq 35°$) for the Op's (a) the case of 1 H-bonded water molecule, (b) the case of two H-bonded water molecules; and (c) the case of three H-bonded water molecules. In (c) due to cylindrical symmetry of the average locations of H-bonded water molecules about P−Op axis, the γ angle is on one of the sides of the tetragon (all H-bond lengths are the same, and the bottom side of the tetragon is an equilateral triangle).

an average of 0.5 and 0.4 H-bonds, respectively, accounting for 9% and 8% of the total number of H-bonds on DMPC (5.3 H-bonds on average). About half of O22 and 30% of O32 H-bonds share water mainly with Op's either of the same (50% O22 and 20% O32) or different (50% O22 and 80% O32) DMPC molecules (Tables 2 and 4, representative conformations in Figures 11c and d). In fact, 66% of intramoelcular bridges involve carbonyl oxygens as one of the end atoms.

Wong and Mantsch[13] showed, using IR spectroscopy, that carbonyl oxygen on the β-chain (O22) exhibited a high level of H-bonding, while that on the γ-chain (O32) does not show any indication of H-bonding. In the present simulation, the level of H-bonding tends to be higher on O22 than O32, but the difference is small. The reason for this discrepancy between results of the experiment and our simulation has not been clarified yet.

The difference in the H-bonding capability of non-ester phosphate and carbonyl oxygens probably arises from (1) the difference in point atomic charges on atoms in both groups[61] and (2) the accessibility of water to the oxygen, i.e., its location in the membrane, since the OPLS energy parameters for the nonbonded interactions are the same for both the non-ester phosphate and carbonyl oxygens. The point atomic charges are much higher on Op's than on the carbonyl oxygens, C═O, partly because the two Op's in DMPC are considered to be two partially ionized sp^2 oxygens that share an extra electron (an extra electron is shared between sp^2 phosphoric oxygen, P═O, and ionized sp^3 phosphate oxygen, P−O−).[61] Thus, the H-bonding is stronger and the number of accepted bonds may be greater for the Op's than those for the Oc's.

With regard to the level of water penetration into the membrane, Figure 8 shows the density profiles of water, non-ester phosphate, and carbonyl oxygens, as well as the choline methyl groups, along the bilayer normal. It is apparent that the carbonyl oxygens are located in a water-deficient region, whereas the choline methyls and phosphate oxygens are well hydrated. The distributions of the numbers of H-bonds per DMPC oxygen are summarized in Figure 9.

5. Intermolecular Bridging. Figure 10 shows the extent of intermolecular water bridging between DMPC molecules in each layer of the membrane at two time points separated by 55 ps (1100 and 1155 ps). The water bridges that lasted longer than 2 ps are shown in these figures. The location of the head group is represented by that of the phosphorus atom. The changes of the locations of the phosphorus atoms are small during the 55 ps. By comparing the intermolecular bridges at these two time points, it is apparent that these bridges are forming and breaking continually. (The lifetimes of H-bonding including intermolecular water bridges will be published elsewhere.) In many cases, two DMPC molecules are simultaneously linked by two, three, and four parallel bridges, which we call double, triple, and quadruple bridging, respectively (four parallel bridges are rare).

Approximately 70% of all DMPC molecules are linked by either single or multiple bridges. However, the bridges do not form extended networks as in the crystal.[2,33] They link DMPC molecules to form local clusters of two to seven molecules. An average of 1.7 H-bonds/DMPC [(1.7/5.3)(100)] = 32% of the total H-bonds on DMPC are involved in either intermolecular or intramolecular bridging (Table 2). Among the H-bonds participating in bridging, 20% are involved in intramolecular bridging (6.4% of the total H-bonds on DMPC) and 80% are involved in intermolecular bridging (25.4% of the total H-bonds on DMPC, Table 2). Therefore, on average 1.4 H-bonds/DMPC are involved in intermolecular bridging (Table 2), which is consistent with the fact that the number of DMPC molecules in one cluster is small. Nevertheless, the number of DMPC molecules linked by water bridges is unexpectedly large.

Representative conformations of single (inter- and intramolecular) and double bridges are shown in Figure 11. Op−Op, Op−Oc, and Op−O11 or O12 bridges account for 55%, 25%, and 12% of the total number of intermolecular bridges, respectively (sum = 92%). The remaining are Oc−Oc (4%) and Oc−O11 or O12 (3%) intermolecular bridges. O22 forms more water bridges than O32, probably because O32 is farther from the head-group atoms than O22. The ester phosphate oxygens (O11 and O12) have practically no contribution to intermolecular bridging (Table 4).

In the DMPC crystal, half of the H-bonded water forms bridges linking O13 of DMPC A with O13 of the previous DMPC B and O14 of DMPC A with O14 of the next DMPC B to form an infinite ribbon along one of the crystalline axes.[2] Water bridges have also been observed between the phosphate groups in cyclopentylphosphorylcholine monohydrate crystal.[62] The major difference in the characteristics of intermolecular bridging in the liquid-crystalline membrane and these crystals is that, in the liquid-crystalline state, H-bonding and water bridging have finite lifetimes due to breaking of H-bonds. The decay time constant of the intermediate component of the H-bond decay, which comprises about 55% of the entire decay process, is on the order of 50 ps (to be published elsewhere). Since orientation and conformation of the head-group moiety of DMPC in the liquid-crystalline phase vary greatly compared

TABLE 2: Numbers of Nearest-Neighbor Water Molecules, H-Bonds Formed Between the Water and DMPC Oxygen Atoms, and H-Bonded Water Molecules in the DMPC Bilayer (Averaged over 500 ps).[a] The Numbers per Oxygen Atom, per Choline Group (Only Nearest Neighbor), and per DMPC Molecule Are Given

	P−O14	P−O13	C═O22	C═O32	P−O11	P−O12	choline	DMPC oxygens (total)
no. of nearest-neighbor water molecules	2.1	2.1	0.6	0.6	0.4	0.3	7.6[b]	4.8 ± 0.2[c]
no. of H-bonds	2.0	2.0	0.5	0.4	0.3	0.1	0	5.3 ± 0.14
% of H-bonds formed on each oxygen	38%	38%	9%	8%	6%	2%		100% (101%)
no. of H-bonded water molecules	1.8	1.7	0.3	0.4	0.2	0.1	0	4.5 ± 0.2
no. of H-bonds involved in bridging DMPC oxygens[d]	0.57	0.59	0.22	0.12	0.12	0.04	0	1.7 ± 0.2
no. of H-bonds involved in intermolecular bridging	0.51	0.51	0.11	0.10	0.10	0.03	0	1.4 ± 0.2
no. of H-bonds involved in intramolecular bridging	0.06	0.08	0.11	0.02	0.02	0.01	0	0.3 ± 0.2

[a] Maximum error in the estimate of the number of H-bonds per atom is ±0.04. Percentages of the shared H-bonds and the shared H-bonded water are 28 ± 4 and 18 ± 4 %, respectively. [b] Water molecules that are H-bonded to P-oxygens are not counted. The value is also corrected for cases in which the same water molecule is the nearest neighbor of other choline methyl groups. [c] Corrected for cases in which the same water molecule is the nearest neighbor of other DMPC oxygens. [d] This number includes H-bonds involved in both intra- and intermolecular bridging.

TABLE 3: Percentage of DMPC Oxygen Atoms Forming Zero, One, Two, Three and Four H-Bonds with Water in the DMPC Bilayer (Averaged over 500 ps). As Shown in Table 2, H-Bonds on Op, C═O22, C═O32, P−O11, and P−O12 Represent 76%, 9%, 8%, 6%, and 2% of the Total Number of H-Bonds on DMPC

no. of H-bonds per oxygen	Op (%)	C═O22 (%)	C═O32 (%)	P−O11 (%)	P−O12 (%)
0	0.5	58	61	72	88
1	20	39	37	27	12
2	58	3	2	1	0
3	21	0	0	0	0
4	0.5	0	0	0	0

with those in the ordered molecular arrays of the crystal, high occurrence of intermolecular water bridges (25.4% of all H-bonds are involved in intermolecular bridging) is surprising. In the DMPC crystal, 67% of H-bonds are involved in intermolecular bridging.

More than half of the H-bridges stay longer than 50 ps, and 10% stay longer than 450 ps, which is still short compared with the lifetimes of the micro clusters of lipids, but comparable to the reorientational correlation time of the head group chain (for example, see ref 18). In addition, no less than 70% of PC's are cross-linked at any instance. Therefore, we suggest that these intermolecular H-bond bridges play important roles in stabilization of the membrane structure.

Many DMPC pairs are connected by multiple parallel water bridges (Figure 10). Of all water bridges, 46% are involved in formation of multiple bridges (i.e., 54% are a sole bridge between the two DMPC molecules). On average, 54%, 40%, 6%, and 0.2% single bridges are involved in single, double, triple, and quadruple bridges, respectively. Multiple parallel bridges consist mainly of Op−Op and Op−Oc bridges, e.g., 74% of double bridges contain these two bridges. In the case of double bridges, Op−Op + Op−Op, Op−Oc + Op−Oc, and Op−Op + Op−Oc account for 41%, 17%, and 16% of double bridges, respectively.

Of all Op−Op bridges, 36% and 31% of all Op−Oc bridges are involved in formation of multiple bridges. Oc−Oc bridges are not involved in formation of multiple parallel bridges.

Double bridges made of two Op−Op bridges are like $O13^1$−water−$O13^2$ + $O14^1$−water−$O14^2$, $O13^1$−water−$O14^2$ + $O14^1$−water−$O13^2$, and $O13^1$−water−$O13^2$ + $O13^1$−water−$O13^2$, in which a double bridge is made between the same two oxygens, and a similar case was found for O14 or $O13^1$−water−$O13^2$ + $O13^1$−water−$O14^2$.

6. Geometry of H-Bonding. Here we present geometric data of water H-bonds accepted by the non-ester phosphate oxygens (Op's: O14 and O13) and carbonyl oxygens (Oc's: O22 and O32). Since the other DMPC oxygens make significantly fewer H-bonds with water, any analysis of these H-bonds is subject to large errors.

6a. H-bonds of Non-Ester Phosphate (Op) and Carbonyl Oxygens (Oc) with Water. Geometry of H-bond is described by 5 parameters in this report: H-bond length and four angles θ, ϕ, β, and γ. The definition of these angles is shown in Figure 12. The average geometries of H-bonds between Op's and water are shown in Figure 13 for the cases in which the oxygens form H-bonds with one, two, or three water molecules. The mean values of these parameters for non-ester phosphate and carbonyl oxygens are summarized in Table 5. Statistical test (Student's *t*-test, $P < 0.05$) indicated that the mean values of these geometric parameters are significantly different for different numbers of H-bonds formed, except β.

For Op's, distributions of ϕ show a shift (Figure 14a) for the cases of one, two, and three H-bonds, while distributions of β for two and three H-bonds nearly overlap. The average value for β is 86° for both two and three H-bond cases, indicating that the preferred geometry of adjacent H-bonds is to form nearly a right angle with each other. We presently do not have an intuitive explanation for preference of this geometry.

γ is an angular parameter that is introduced to monitor variations between planar trigonal geometry ($\gamma = 0°$) and steric tetragonal geometry ($\gamma = 45°$, in a case when $\beta = 90°$ and $\phi = 125°$) (see Figures 12 and 13). The distributions of γ are shown in Figure 15a in the presence of two and three H-bonded water molecules to Op's. In the presence of two H-bonded water molecules, the average γ is zero degrees, but the distribution is quite broad (Figure 15a). This result suggests that, on average, the Op and two water oxygen atoms lie in one plane, like an sp^2 orbital. However, since ϕ and β angles are quite different from 120°, the geometry is not a regular trigonal one. In addition, the broad distribution of γ suggests that even in the presence of two H-bonded water molecules, the locations of many water molecules are close to those in the tetragonal distribution found in the presence of three H-bonded water molecules.

In the presence of three H-bonded water molecules, the average of the absolute value of γ is 40° (the maximum of $|\gamma|$ distribution is ≈45°), indicating tetragonal geometry for Op and three water oxygens, like an sp^3 orbital. If we assume that the three water oxygens occupy cylindrically symmetric locations with respect to the Op, and that $\beta = 90°$, then $\phi = 125°$ and $\gamma = 45°$. The actual average value of ϕ is 126°, indicating a good tetragonal symmetry in the case of three H-bonded water molecules.

TABLE 4: Percentage of H-Bonds Involved in Inter- and Intramolecular Bridging (Averaged over 500 ps)

A. Percentages of H-Bonds Involved in Intermolecular Bridging with Respect to the Total Number of H-Bonds Formed on a DMPC Oxygen[a]

oxygen atom	% against no. of total H-bonds on the atom	target oxygen on the other end of the H-bonded water bridge					
		P−O14	P−O13	C═O22	C═O32	P−O11	P−O12
P−O14	28	43	28	12	6	9	2
P−O13	33	24	42	18	10	3	3
C═O22	44	32	56	4	1	5	2
C═O32	31	26	47	9	11	6	1
P−O11	40	46	20	9	8	9	8
P−O12	38	29	40	11	2	19	0

B. Ratio of Intermolecular/Intramolecular Bridging (%, Rounded to 5%)

oxygen atom	P−O14	P−O13	C═O22	C═O32	P−O11	P−O12
P−O14	100/0	100/0	50/50	80/20	80/20	65/35
P−O13		100/0	50/50	80/20	80/20	65/35
C═O22			100/0	90/10	60/40	40/60
C═O32				100/0	100/0	0/0
P−O11					100/0	80/20
P−O12						0/0

[a] Total number of H-bonds formed on a DMPC oxygen is shown in the first column. Percentages of those forming intermolecular bridging are shown in the second column. The intermolecular bridges are further classified according to the other side of the bridge with respect to the total number of water bridges formed on the DMPC oxygen.

TABLE 5: H-Bonding Geometry for One, Two, and Three H-Bonds between Water and DMPC Oxygens (Averaged over 200 ps for Pure Water and over 500 ps for Water in the Membrane System, Mean ± SD). Percentages in Parentheses Show the Fractions of Op's that Form One, Two, and Three H-Bonds. The Numbers in This Table Include Both Bridging and Nonbridging Cases

	H-bond length (Å)	θ (deg)	ϕ (deg)	β (deg)	γ (deg)
a. Op (4.0 H-Bonds/DMPC)					
1 H-bond (20%)	2.66 ± 0.12	10.2 ± 6	142 ± 17	ND[a]	ND
2 H-bonds (58%)	2.71 ± 0.14	11.7 ± 7	132 ± 16	86 ± 15	0.1 ± 31
3 H-bonds (21%)	2.78 ± 0.17	13.2 ± 8	126 ± 16	86 ± 17	40 ± 19
b. C═O22 (0.5 H-Bonds/DMPC)					
1 H-bond (39%)	2.83 ± 0.16	16.5 ± 8	140 ± 17	ND	ND
2 H-bond (3%)	2.89 ± 0.18	17.9 ± 9	133 ± 16	85 ± 18	0.0 ± 32
c. C═O32 (0.4 H-Bonds/DMPC)					
1 H-bond (37%)	2.84 ± 0.16	16.6 ± 8	139 ± 17	ND	ND
2 H-bond (2%)	2.90 ± 0.18	17.7 ± 9	131 ± 17	82 ± 17	0.8 ± 34

[a] ND = not defined.

The average length of the H-bond tends to increase slightly with an increase in the number of H-bonded water molecules (Table 5, *t*-test: $P < 0.05$).

In the case of carbonyl oxygens, i.e., O22 and O32, up to two H-bonds are formed with water (Table 3). In a screening of crystallographic data, one, two, and three H-bonds are reportedly accepted by the C═O group, but cases with three H-bonds are rare.[63] The distributions of θ, ϕ, β, and γ are similar for O22 and O32, and therefore, the average distributions for O22 and O32 are shown in Figures 14b (θ, ϕ, and β) and 15b (γ).

The shapes of distributions of these geometry parameters for carbonyl oxygens are similar to those found for non-ester phosphate oxygens (compare Figures 14a,b). However, the mean values of θ and ϕ (Table 5) are significantly different from those for Op (*t*-test: $P < 0.05$). Similarities in distributions of β and γ for both Op's and O's indicate that, for the case of two H-bonds, their H-bond geometries are planar trigonal. The H-bonds are slightly longer for the carbonyl oxygens than for non-ester phosphate oxygens, which is consistent with crystallographic data[62−64] and smaller partial atomic charges (see Table 1).

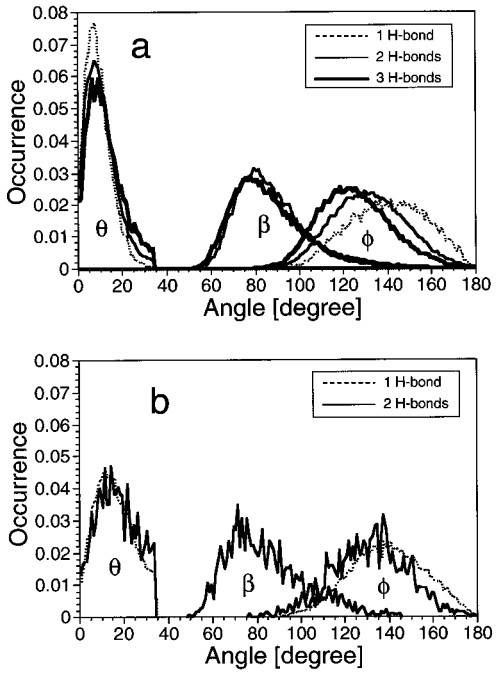

Figure 14. Distributions of θ, β, and ϕ for the cases of one H-bonded water molecule (dot line), two H-bonded water molecules (thin solid line), and three H-bonded water molecules (thick solid line): (a) Op's, (b) Oc's (both O22 and O32, the cases of one and two H-bonded water molecules only).

In a DMPC crystal, four water molecules form six H-bonds with the Op's of two DMPC molecules.[2,34,64] Two water molecules form intermolecular bridges between two DMPC molecules (thus form four H-bonds with Op's), and two water molecules form one H-bond each. H-bond angles and length in the energy-minimized structure of the DMPC crystal[34] are summarized in Table 6. The distributions of H-bond angles obtained in this simulation of the liquid-crystalline membrane include those determined in the crystal (Figure 14a). The following points are noted. (1) The broad distribution of β may be due to superposition of distributions of β around the two values found in the crystal. (2) The average θ's are 12° and 17° for phosphate and carbonyl oxygens, respectively, which is within the limit of about 20° encountered experimentally in H-bonding.[58] (3) The H-bond length is preserved both in the

TABLE 6: H-Bonding Geometry of Op for One, Two, and Three H-Bonds with Water (Averaged over 500 ps, Mean ± SD) for the Case of Bridging[a]

	H-bond length (Å)	θ (deg)	ϕ (deg)	β (deg)	γ (deg)
		a. H-Bonds Involved in Intermolecular Bridging			
1 H-bond (10%)	2.69 ± 0.12	10.3 ± 6	144 ± 17	ND[b]	ND
2 H-bonds (76%	2.72 ± 0.15	11.7 ± 7	131 ± 16	86 ± 14	−0.1 ± 31
3 H-bonds (14%)	2.78 ± 0.17	13.5 ± 7	125 ± 15	86 ± 16	40 ± 19
		b. H-Bonds Not Involved in Any Bridging			
1 H-bond (21%)	2.66 ± 0.12	10.2 ± 6	142 ± 17	ND	ND
2 H-bonds (57%)	2.71 ± 0.14	11.7 ± 7	132 ± 16	87 ± 15	0.2 ± 31
3 H-bonds (22%)	2.78 ± 0.17	13.3 ± 8	126 ± 16	86 ± 17	40 ± 19
		c. P-Oxygens, Crystal[c]			
nonbridging H-bonds	2.66	9.8	123.1	ND	ND
	2.65	15.9	157.8	ND	ND
bridging H-bonds	2.59	10.2	109.4	60.4	−18.5
	2.63	11.0	122.6	86.6	17.4
	2.68	18.8	136.2	n.d.	22.2
	2.70	24.9	140.6	n.d.	−43.7

[a] Oc−Oc inter- and intramolecular bridges are rare and Op−Op intramolecular bridges did not take place. Therefore, only Op−Op intermolecular bridges are analyzed in this table. (19% and 0.1% of Op's are involved in Op−Op inter- and intramolecular bridging, respectively. Table 4A shows that 28% of Op14 and 33% of Op13 are involved in Op−Op, Op−Oc, and Op−ester phosphate oxygen bridges.) Percentages shown in parentheses in (a) and (b) show the fractions of Op's that form one, two, and three H-bonds (total number of H-bonds on the Op) with respect to the total number of Op's that are (a) and are not (b) involved in intermolecular bridging. [b] ND = not defined. [c] In DMPC−$2H_2O$ crystal.[34] In the DMPC crystal, four water molecules from six H-bonds with the Op's of two DMPC molecules.[34,64] Two water molecules are involved in cross-bridges between two DMPC molecules (thus form four H-bonds), and two water molecules form one H-bond each.

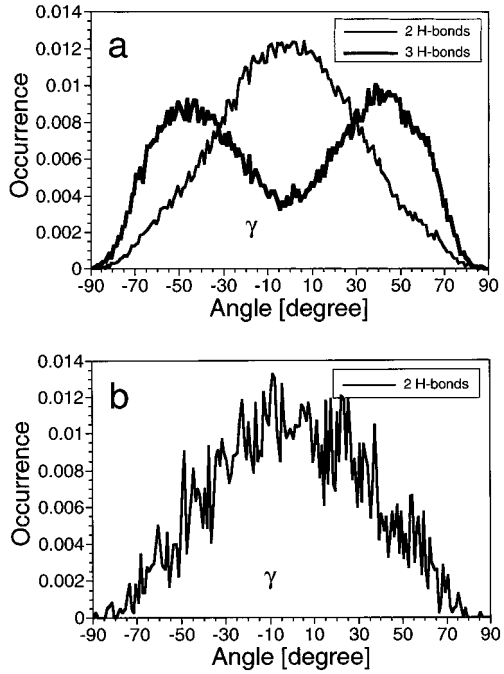

Figure 15. Distributions of γ for (a) Op's for the cases of two H-bonded water molecules (thin solid line) and three H-bonded water molecules (thick solid line), as well as (b) Oc's (the case for two H-bonded water molecules only).

crystal and in the liquid-crystalline state. In addition, similar H-bond length was found in phosphorylcholine hydrate crystal.[62]

Both theoretical (for example, ref 65 and references therein) and experimental[66,67] studies indicate that H-bonding occurs preferentially in the direction of the lone pair orbitals. However, this anisotropy is not very pronounced.[58] Although both phosphoryl and carbonyl oxygens have two sp^2 lone pairs, each oriented 120° from the C═O or P═O bond, the average ϕ that is most often encountered in crystallographic data is 135° with a range of 90° to 180° (for example,[58,64,68]), which is similar to the ϕ observed here (132° and 139° for phosphate and carbonyl oxygens, respectively, Table 6) and to the range of the distribution of ϕ observed in the present work.

TABLE 7: H-Bonding Geometry for One, Two, and Three H-Bonds in Water−Water H-Bonds (Averaged over 200 ps, Mean ± SD)

	H-bond length (Å)	θ (deg)	ϕ (deg)	β (deg)	γ (deg)
1 H-bond (30%)	2.81 ± 0.17	13.9 ± 7.7	120 ± 21	ND[a]	ND
2 H-bonds (57%)	2.90 ± 0.21	15.9 ± 8.4	114 ± 24	89 ± 20	50 ± 21
3 H-bonds (12%)	2.99 ± 0.23	18.2 ± 9.0	111 ± 28	92 ± 26	43 ± 24

[a] ND = not defined.

6b. Geometry of Bridging and Nonbridging Water. Geometries of H-bonds that are involved in intermolecular bridging are compared with those that are involved in neither intermolecular nor intramolecular bridging for the case of Op−Op intermolecular bridging (Table 6). Other types of bridges occur less often and could not be analyzed in a meaningful way. The distributions and the mean values of θ, ϕ, β, and γ are similar between H-bonds involved and not involved in bridging for each case of one, two, and three H-bonds formed ($P < 0.05$, *t*-test). Only H-bond lengths in the cases of one and two H-bonds are slightly different between bridging and nonbridging bonds. These results suggest that bridging H-bonds are formed without causing distortion in the geometry of the H-bonds.

6c. Comparison of H-Bond Geometries between Op (Non-Ester Phosphate Oxygen) and Ow (Water Oxygen). Both Ow and Op can make one, two, and three H-bonds with water, and both preferentially make two H-bonds (about 60%, Tables 5 and 7). Neutron diffraction studies on water have indicated that an average of two water molecules are accepted by the water oxygen.[67] Monte Carlo simulations for liquid water also indicate that two is the most probable number of H-bonds per water oxygen.[36] Our results agree well with these results.

Parameters of H-bond geometries (H-bond length, θ, ϕ, β, and γ) are summarized in Tables 5 and 7 for Op and Ow, respectively. All these parameters are significantly different between Op and Ow when they are compared for the same number of H-bonds formed (*t*-test, $P < 0.01$). H-bond geometry varies as the number of H-bonds formed changes from one to three (significant difference according to the *t*-test with $P < 0.01$) in both cases of Op and Ow, and the ways of their changes are similar for both cases (see Tables 5 and 7), except γ.

γ's of Ow and Op are very different in the case of two H-bonds: their mean values are 50° for Ow and 0° for Op. In the case of Ow, γ is not far from 45° for both two and three H-bond cases, indicating that water−water hydrogen bonds are always steric tetragonal. In the case of Op, H-bond geometry is planar trigonal for two H-bonds, while it is steric tetragonal for three H-bonds.

Average H-bond length is greater in water−water than in Op−water H-bonds. Longer bonds for water−water H-bonding were anticipated from the comparison of RDFs of water oxygens relative to P- and water oxygens (Figure 6e). (The H−Ow···Ow angle ϕ for water−water H-bonds should be close to the tetrahedral angle of 109.5°; in this simulation it is 114°. Although the results of ab initio calculations[69] do not indicate any distinct minima for tetrahedral orientation angles in water dimers, experimental results show that liquid water molecules have tetrahedral H-bonding.[66,67]) These results suggest that water−Op H-bonding is stronger than water−water H-bonding. This might explain the readiness with which water forms H-bonds with Op, and therefore, frequent Op−Op bridges.

7. Geometry of Water Ordered by the Choline Group. The shape of the RDF of water oxygens relative to the choline methyl groups indicates that, although the groups are not able to form H-bonds with water, they significantly order nearby water (Figure 6d). Water molecules whose oxygen atoms are located within 4.75 Å from the methyl group (position of the first minimum in the RDF in Figure 6d), and which are also not H-bonded to any Op, are considered to comprise the hydration shell. The positions of the first peaks in the RDF's of the water hydrogens and water oxygens relative to NCH_3 overlap very well, implying that one of the water hydrogen atoms is almost at the same distance from NCH_3 as the oxygen atom. Indeed, the distribution of the NCH_3···Ow−H angle for the NCH_3 hydration shell water has a maximum at about 76° and a shoulder at about 130°−140°. In addition, the average angle between the water dipole and the NCH_3···Ow vector is about 103 ± 26°. These findings confirm that the average orientation of water from the choline hydration shell is such that one of the Ow−H bonds is almost tangent to, and the other Ow−H bond makes an angle of about 130° with the NCH_3···Ow vector. This orientation is typical of the clathrate structure formed by water around a nonpolar moiety.[70]

A similar ordering of water has been reported by Alper et al.[23] in the DMPC monolayer generated by MD simulation. The ordering was seen more clearly in their simulation: the two peaks in the distribution of the NCH_3···Ow−H angle were better separated than in our system, probably because they used an all-atom model for DMPC, while we used a united atom approximation.

Conclusions

Several conclusions can be drawn: (1) A stable computer model of a fully hydrated DMPC bilayer in the liquid-crystalline state was generated. The surface area per DMPC (61 ± 1 Å^2), the number of gauche conformations in the hydrocarbon chain of DMPC (2.9/chain), and the profile of the order parameter of the simulated membrane are in basic agreement with those found experimentally. It is concluded that this computer model adequately reproduces features of the DMPC bilayer membrane.

(2) In the simulated membrane, 5.3 H-bonds are formed per DMPC between water and DMPC oxygens; 4 of these bonds involve non-ester phosphate oxygens, 0.9 involve carbonyl oxygens, and the remaining bonds involve ester phosphate oxygens.

(3) An important finding in this work, which is not easy to show experimentally but is apparent in the simulation, is that, even in the liquid-crystalline membrane, many water bridges are formed between DMPC molecules to generate clusters. Approximately 70% of DMPC molecules are linked by single or multiple water bridges and form clusters of two to seven molecules.

(4) Both oxygen of Op and water in the bulk phase (Ow) form two H-bonds most often (≈60%). In the case of two H-bonds formed on Op or Oc, the geometry of H-bonding is planar trigonal. When Op forms three H-bonds, geometry of H-bonding is steric tetragonal. In the case of Ow, geometry is always steric tetragonal.

(5) On average, the H-bonds form nearly right angles with each other when two or three water molecules are bound to the same DMPC oxygen, but the distribution of the angle is broad.

Acknowledgment. We would like to thank Shigeyuki Sumiya and Koji Oda for their helpful discussion. This work was supported in part by a grant from The Polish Science Foundation (Grant BIMOL 103/93), by a special promotion fund from the Science and Technology Agency, and by grants-in-aid from the Ministry of Education, Science, and Culture of Japan.

References and Notes

(1) Tanford, C. *The Hydrophobic Effect*; Wiley: New York, 1980.
(2) Pearson, R. H.; Pascher, I. *Nature*; **1979**, *281*, 499−501.
(3) Hauser, H.; Pascher, I.; Pearson, R. H.; Sundell, S. *Biochim. Biophys. Acta*; **1981**, *650*, 21−51.
(4) Griffith, O. H.; Dehlinger, P. J.; Van, S. P. *J. Memb. Biol.* **1974**, *15*, 159−192.
(5) Weaver, J. C.; Powell, K. T.; Mintzer, R. A. *Bioelectrochem. Bioenerg.* **1984**, *12*, 405−412.
(6) Nagle, J. F. *Bioelectrochem. Bioenerg.* **1987**, *19*, 413−426.
(7) Deamer, D. W.; Nichols, J. W. *J. Membr. Biol.* **1989**, *107*, 91−103.
(8) Subczynski, W. K.; Wisniewska, A.; Yin, J.-J.; Hyde, J. S.; Kusumi, A. *Biochemistry* **1994**, *33*, 1670−1681.
(9) Helfrich, W.; Servuss, R.-M. *Nuovo Cimento Soc. Ital. Fis., D* **1984**, *3*, 137−151.
(10) Gawrisch, K.; Arnold, K.; Gottwald, T.; Klose, G.; Volke, F. *Stud. Biophys.* **1978**, *74*, 13−14.
(11) Arnold, K.; Pratsch, L.; Gawrisch, K. *Biochim. Biophys. Acta* **1983**, *728*, 121−128.
(12) Nagle, J. F. *Biophys. J.* **1993**, *64*, 1476−1481.
(13) Wong, P. T. T.; Mantsch, H. H. *Chem. Phys. Lipids* **1988**, *46*, 213−224.
(14) Wu, S. H.; McConnell, H. M. *Biochemistry* **1975**, *14*, 847−854.
(15) Karnovsky, M. J.; Kleinfeld, A. M.; Hoover, R. L.; Klausner, R. D. *J. Cell Biol.* **1982**, *94*, 1−6.
(16) Sackmann, E.; Ruppel, D.; Gebhardt, C. In *Liquid Crystals of One- and Two-Dimensional Order*; Helfrich, W., Heppke, G., Eds.; Springer Verlag: Berlin, 1982; pp 309−326.
(17) Meirovitch, E.; Freed, J. H. *J. Phys. Chem.* **1980**, *84*, 3281−3295.
(18) Subczynski, W. K.; Antholine, W. E.; Hyde, J. S.; Kusumi, A. *Biochemistry* **1990**, *29*, 7936−7945.
(19) Charifson, P. S.; Hiskey, R. G.; Pedersen, L. G. *J. Comput. Chem.* **1990**, *11*, 1181−1186.
(20) Berkowitz, M. L.; Raghavan, K. *Langmuir* **1991**, *7*, 1042−1044.
(21) Raghavan, K.; Reddy, M. R.; Berkowitz, M. L. *Langmuir* **1992**, *8*, 233−240.
(22) Damodaran, K. V.; Merz, K. M., Jr.; Gaber, B. P. *Biochemistry* **1992**, *31*, 7656−7664.
(23) Alper, H. E.; Bassolino-Klimas, D.; Stouch, T. R. *J. Chem. Phys.* **1993**, *99*, 5547−5559.
(24) Damodaran, K. V.; Merz, K. M., Jr. *Biophys. J.* **1994**, *66*, 1076−1087.
(25) Marrink, S.-J.; Berendsen, H. J. C. *J. Phys. Chem.* **1994**, *98*, 4155−4168.
(26) Egberts, E.; Marrink, S.-J.; Berendsen, H. J. C. *Eur. Biophys. J.* **1994**, *22*, 423−436.
(27) Kusumi, A.; Subczynski, W. K.; Pasenkiewicz-Gierula, M.; Hyde, J. S.; Merkel, H. *Biochim. Biophys. Acta* **1986**, *854*, 307−317.
(28) Kusumi, A.; Pasenkiewicz-Gierula, M. *Biochemistry* **1988**, *27*, 4407−4415.
(29) Pasenkiewicz-Gierula, M.; Subczynski, W. K.; Kusumi, A. *Biochemistry* **1990**, *29*, 4059−4069.

(30) Pasenkiewicz-Gierula, M.; Subczynski, W. K.; Kusumi, A. *Biochimie* **1991**, *73*, 1311−1316.
(31) Subczynski, W. K.; Hyde, J. S.; Kusumi, A. *Proc. Natl. Acad. Sci. U.S.A.* **1989**, *86*, 4474−4478.
(32) Subczynski, W. K.; Hyde, J. S.; Kusumi, A. *Biochemistry* **1991**, *30*, 8578−8590.
(33) Pearlman, D. A.; Case, D. A.; Caldwell, J. C.; Seibel, G. L.; Singh, U. C.; Weiner, P. K.; Kollman, P. A. AMBER 4.0; University of California, San Francisco, 1991.
(34) Vanderkooi, G. *Biochemistry* **1991**, *30*, 10760−10768.
(35) Jorgensen, W. L.; Tirado-Rives, J. *J. Am. Chem. Soc.* **1988**, *110*, 1657−1666.
(36) Jorgensen, W. L.; Chandrasekhar, J.; Madura, J. D.; Impey, R.; Klein, M. L. *J. Chem. Phys.* **1983**, *79*, 926−935 and references therein.
(37) Frisch, M. J.; Head-Gordon, M.; Trucks, G. W.; Foresman, J. B.; Schlegel, H. B.; Raghavachari, K.; Robb, M. A.; Blinkley, J. S.; Gonzalez, C.; Defrees, D. J.; Fox, D. J.; Whiteside, R. A.; Seeger, R.; Melius, C. M.; Baker, J.; Martin, R. L.; Kahn, L. R.; Stewart, J. J. P.; Topiol, S.; Pople, J. A. GAUSSIAN-90; Gaussian, Inc.: Pittsburgh, PA, 1990.
(38) Connolly, M. L. *Science* **1983**, *221*, 709−713.
(39) Ryckaert, J. P.; Cicotti, G.; Berendsen, H. J. C. *J. Comput. Phys.* **1977**, *22*, 327−341. Chiu, S.-W.; Clark, M.; Balaji, V.; Subramanian, S.; Scott, H. L.; Jacobsson, E. *Biophys. J.* **1995**, *69*, 1230−1245.
(40) Egberts, E.; Marrik, S.-J.; Berendsen, H. C. *Eur. Biophys. J.* **1994**, *22*, 432−436.
(41) Ewald, P. P. *Ann. Phys.* **1921**, *64*, 253−287.
(42) Berendsen, H. J. C.; Postma, J. P. M.; van Gunsteren, W. F.; DiNola, A.; Haak, J. R. *J. Chem. Phys.* **1984**, *81*, 3684−3690.
(43) Stouch, T. R.; Williams, D. E. *J. Comput. Chem.* **1992**, *13*, 622−632.
(44) Mendelsohn, R.; Davies, M. A.; Brauner, J. W.; Schuster, H. F.; Dluhy, R. A. *Biochemistry* **1989**, *28*, 8934−8939.
(45) Salsbury, N. J.; Darke, A.; Chapman, D. *Chem. Phys. Lipids* **1972**, *8*, 142−151.
(46) Rand, R. P.; Parsegian, V. A. *Biochim. Biophys. Acta* **1989**, *988*, 351−376.
(47) Nagle, J. F.; Wiener, M. C. *Biochim. Biophys. Acta* **1988**, *942*, 1−10. Nagle, J. F.; Zhang, R.; Tristram-Nagle, S.; Sun, W.; Petrache, H. I.; Suter, R. M. *Biophys. J.* **1996**, *70*, 1419−1431. Tu, K.; Tobias, D. J.; Klein, M. L. *Biophys. J.* **1995**, *69*, 2558−2562.
(48) Pink, D. A.; Green, T. J.; Chapman, D. *Biochemistry* **1980**, *19*, 349−356.
(49) Casal, H. L.; McElhaney, R. N. *Biochemistry* **1990**, *29*, 4523−5427.
(50) Seelig, A.; Seelig, J. *Biochemistry* **1977**, *16*, 45−50.
(51) Hubbell, W. L.; McConnell, H. M. *J. Am. Chem. Soc.* **1971**, *93*, 314−326.
(52) Meier, P.; Blume, A.; Ohmes, E.; Neugebauer, F. A.; Kothe, G. *Biochemistry* **1982**, *21*, 526−534.
(53) Moser, M.; Marsh, D.; Meier, P.; Wassmer, K.-H.; Kothe, G. *Biophys. J.* **1989**, *55*, 111−123.
(54) Carlson, J. M.; Sethna, J. P. *Phys. Rev. A* **1987**, *36*, 3359−3374.
(55) Büldt, G.; Gally, H. U.; Seelig, J. *J. Mol. Biol.* **1979**, *134*, 673−691.
(56) Levine, Y. K.; Wilkins, M. H. F. *Nature New Biol.* **1971**, *230*, 69−72.
(57) Stouch, T. R. *Mol. Simul.* **1993**, *10*, 335−362.
(58) Murray-Rust, P.; Glusker, J. P. *J. Am. Chem. Soc.* **1984**, *106*, 1018−1025.
(59) Borle, F.; Seelig, J. *Biochim. Biophys. Acta* **1983**, *735*, 131−136.
(60) Frischleder, F.; Gleichmann, S.; Karhl, R. *Chem. Phys. Lipids* **1977**, *19*, 144−149.
(61) Vanderkooi, G. *J. Phys. Chem.* **1983**, *87*, 5121−5129.
(62) Sarma, R.; Ramirez, F.; Narayanan, P.; McKeever, B.; Okazaki, H.; Marecek, J. F. *J. Am. Chem. Soc.* **1978**, *100*, 4453−4458.
(63) Taylor, R.; Kennard, O.; Versichel, W. *J. Am. Chem. Soc.* **1983**, *105*, 5761−5766.
(64) Vanderkooi, G. *Biochemistry* **1991**, *30*, 10760−10768 (Supplementary Material).
(65) Scheiner, S. In *Reviews in Computational Chemistry II*; Lipkowitz, K. B., Boyd, D. B., Eds.; VCH Publishers, Inc.: New York, 1991; pp 165−218.
(66) Narten, A. H.; Levy, H. A. *Science* **1969**, *165*, 447−454.
(67) Narten, A. H.; Thiessen, W. E.; Blum, L. *Science* **1982**, *217*, 1033−1034.
(68) Vedani, A.; Dunitz, J. D. *J. Am. Chem. Soc.* **1985**, *107*, 7653−7658.
(69) Stillinger, F. H. *Science* **1980**, *209*, 451−457 and references therein.
(70) Alper, H. E.; Bassolino, D.; Stouch, T. R. *J. Chem. Phys.* **1993**, *98*, 9798−9807.